UCRL-97082
PREPRINT

DETAILED KINETIC MODELING OF AUTOIGNITION CHEMISTRY

Charles K. Westbrook
William J. Pitz

This paper was prepared for submittal to
1987 International Fuels & Lubricants Meeting
and Exposition, Toronto, Ontario
November 2-5, 1987

July 22, 1987

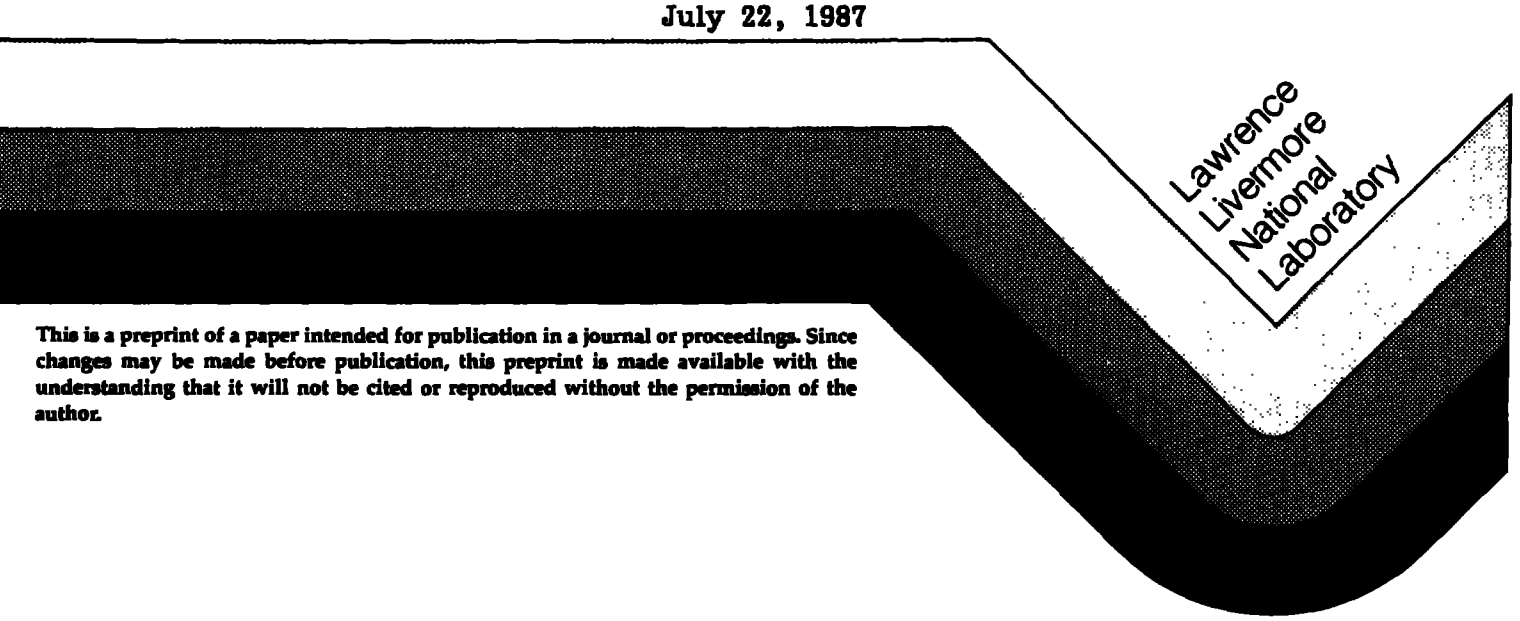

DETAILED KINETIC MODELING OF AUTOIGNITION CHEMISTRY

Charles K. Westbrook and William J. Pitz
Lawrence Livermore National Laboratory, Livermore, California 94550

Abstract

The development of detailed chemical kinetic reaction mechanisms for analysis of autoignition and knocking of hydrocarbon fuels is described. In particular, kinetic processes of concern for the oxidation of complex hydrocarbon fuel molecules are emphasized. The wide ranges of temperature and pressure which are encountered by end gases in automobile engine combustion chambers result in extreme demands on reaction mechanisms which are intended to describe knocking conditions and predict rates of combustion and ignition. The reactions and chemical species which are most important in each temperature and pressure regime are discussed, and the validation of these reaction mechanisms through comparison with idealized experimental results is described.

KINETIC MODELS OF AUTOIGNITION have been used in recent years to assist in the understanding of the chemical processes which take place in the combustion chamber of an internal combustion engine. In particular, autoignition plays a large role in the problem of engine knock. The degree of kinetic sophistication can vary widely from one model to another, depending on the way in which that model is intended to be integrated into the overall description of the engine combustion problem and on the amount of kinetic information which is available for the specific hydrocarbon fuels being considered.

In the past, perhaps the most fruitful type of kinetics modeling for autoignition and engine knock has followed the approach of the so-called Shell Model [1-3], which used a type of generalized reaction mechanism. The major kinetic processes in the Shell Model are all based on actual reactions observed in the lower temperature oxidation of hydrocarbon fuels. Most important, the principal chain branching mechanism in the Shell Model involves the addition of molecular oxygen to the (alkyl) radical, followed by degenerate chain branching and leading to a thermal explosion. Other important steps include internal H atom abstraction (alkyl peroxy isomerization), and formation of dihydroperoxy radicals. In all of these cases, the production of OH radicals is a very important output quantity. The Shell Model and others based upon it [e.g. 4,5] have been very successful in many cases at helping to describe the dependence of engine knock on engine operating parameters.

A parallel development effort over the past several years [6-9] has emphasized a more detailed chemical kinetic modeling approach than that included in the Shell Model. Although more costly in terms of development time and requiring more powerful computational resources, these detailed models promise an improved ability to treat such effects as fuel molecular structure, mixtures of fuels, and the use of fuel additives. In the Shell Model, the global or representative reactions have rates which have to be adjusted for each fuel to be analyzed, a process which requires extensive experimental testing of each fuel. In contrast, a detailed kinetic model must use reaction rate data which are more fundamentally based than those in a more global model. In addition, these models must be orders of magnitude larger and more complex than global models. The current research which is being carried out in moving towards such a goal is described in this paper, along with some of the accomplishments of this type of approach.

OVERALL END GAS HISTORY

A typical engine cycle begins when unburned fuel and air are introduced into the combustion chamber. This charge is compressed by the piston and spark-ignited at a time usually close to top-dead-center (TDC). A flame then begins to propagate across the chamber, steadily converting fuel and air to combustion products. The gases which have not yet been consumed (the "end gases") are not chemically inert during this time interval; they are reacting steadily but at rather low rates. Under normal operation, the end gases are consumed by the flame propagating through the engine chamber. However, under extreme conditions of high pressure and/or temperature, it is possible for these end gases to autoignite spontaneously prior to the arrival of the flame. When autoignition produces a sufficiently rapid pressure rise and involves a significant fraction of the end gas, engine knock results. The objective of the present study is to identify the chemical kinetic mechanisms which lead to autoignition.

Temperature History

During the combustion of the fuel-air mixture in a typical spark ignition engine, the unburned portion of the charge is subjected to a considerable increase in pressure and temperature as a result of compression, both by the engine piston and by the expansion of the burned product gases. As a result, the kinetic pathways which control the rate of reaction can also change drastically. Three temperature regimes can be defined which cover the temperature history of the end gas. The chemical kinetic features of each of these regimes will be discussed later in this paper. The first kinetic regime encountered by the end gas is at low

temperature. At the time when the intake valve opens, the unburned mixture is at approximately atmospheric temperature and pressure. As the end gas is compressed by the piston, it spends a large fraction of its time in the temperature range from 450 K to about 800 K; at low engine speeds, the end gases may be in this range for as long as 70 ms [7-9]. Although the overall rate of combustion is quite slow in this temperature range, the residence time is long enough for some fuel consumption and heat release to occur.

As the temperature of the end gas increases above about 800 - 850 K, the dominant kinetic paths change markedly. At the lower temperatures, the overall reaction takes place primarily through the formation of various alkylperoxy radicals via addition of molecular oxygen to alkyl radicals, followed by production of alkyl hydroperoxides which then decompose to produce OH radicals and various oxygenated hydrocarbon species. At higher temperatures, however, the alkylperoxy radicals become unstable, resulting in a region of negative temperature coefficient, and the lower temperature reaction paths are no longer observed. Instead, the combustion becomes controlled by the reactions of the hydroperoxyl radical and hydrogen peroxide.

As the temperature increases further to values above about 1100-1200K, the dominant reaction path changes again, being controlled by the production of H atoms which then react with molecular oxygen to produce both oxygen atoms and OH radicals. The crossover into the highest temperature regime, where H atom kinetics replace HO_2 kinetics, is influenced by the system pressure as well as the temperature. At the relatively high pressures encountered in the end gases of internal

combustion engines, this transition regime is found around 1200 K as already noted, but at atmospheric pressure it is seen to occur at about 1000 K.

The problem of modeling the chemical kinetics of end gas autoignition is considerably more difficult than modeling the kinetics of most other types of experiments because the end gases spend significant fractions of their time in all of these temperature regimes, and the kinetic model must be able to describe all of the important reaction paths and rates in each regime. As we will discuss below, high accuracy is required of the predictions, particularly with regard to heat release rates during the lower temperature ranges.

The time history of the end gas temperature is illustrated schematically in Fig. 1 as a function of engine crank angle (or time). These curves are based on earlier experimental and modeling work in which the end gas temperatures were either measured directly or calculated from the engine pressure history [7-9]. The solid curve shows the temperature for a case where knock does not occur, since the flame arrival takes place before the onset of autoignition. The dashed curve shows the temperature for a case in which knock is observed, where the ignition occurs before the time of flame arrival. In this illustration, the two cases are assumed to ignite at effectively the same temperature T_1; a considerable body of experimental evidence [7,10] suggests that the autoignition temperature is a relatively weak function of engine operating conditions, and kinetic reasons supporting this point will be presented later. In Fig. 1 it is apparent that the difference between the two cases (i.e. knocking vs. non-knocking) is the result of an accumulated difference in the rates of heat release over the entire end gas history.

further point is that the differences in temperature between the two curves are quite modest; an estimate of a ±30K temperature differential is shown in Fig. 1. This small temperature differential causes the case with the dashed curve to reach the ignition temperature T_1 at an earlier time than the case shown by the solid curve, and thus the former case exhibits knocking.

We will return to Fig. 1 in the discussions to follow. For the present, in terms of the discussion of the various temperature regimes outlined above, it should be apparent that any numerical model of the chemical kinetics of the end gas oxidation must be able to predict small amounts of heat release over an extended range of end gas temperatures, a range that covers all of the kinetic pathways to be described in detail below.

Fuel Structure

Another significant degree of difficulty in modeling the autoignition of typical hydrocarbon fuels under knocking conditions is due to the actual composition of the fuel itself. Conventional automotive fuel is usually a complex mixture of different constituents, including saturated and unsaturated straight and branched chain species as well as aromatic and other types of molecular structures. Very few of these species have been described by detailed chemical kinetic reaction mechanisms in <u>any</u> of the temperature and pressure regimes which are important for knock.

Three sets of examples will be used to illustrate the descriptions to follow. In Fig. 2 are shown two isomeric forms of octane, the straight chain molecule n-octane and the branched chain form, iso-octane, also referred to as 2-2-4 trimethyl pentane. For reasons which will become

clear very shortly, the H atoms in the n-octane figure have been indicated by numerals 1 through 4. For similar reasons, the H atoms in iso-octane are denoted by the letters a, b, c, and d. Both fuels have the same numbers of C and H atoms, both have very nearly the same heat of reaction, and the burning velocities of flames through mixtures of both fuels with air are very similar. However, the autoignition properties of the two fuels are dramatically different. The octane number of a given fuel is a measure of its autoignition rate and tendency to knock under engine conditions, with a large number indicating good resistance to knock and a small number indicating a tendency to knock. Iso-octane is very knock-resistant; its octane number is equal to 100, and iso-octane is used to define this point on the octane scale. On the other hand, n-octane has a very high knock tendency, with an octane number less than zero (the smaller fuel n-heptane has, again by definition, an octane number of exactly zero, and n-octane is slightly more prone to knock than is n-heptane). Therefore, the vast difference in knocking tendency for these fuels can be attributed only to the differences in the structure of the two molecules. Octane ratings in this study are taken from several sources [11,12].

The same type of structural differences can be seen in Fig. 3 for the two isomeric forms of butane, the straight chain form n-butane, and the branched iso-butane. While there are many isomers of octane (with only two of them shown in Fig. 2), these are the only two forms for butane, and the effects of structure can be studied even more directly. Again, the flame temperatures and burning velocities for the two fuels are very similar. The differences in octane number and autoignition rate are not as great as for the octanes, but the differences are still significant.

The octane number for iso-butane is 100 (defined as the average of the research and motored octane numbers), while that of n-butane is 92, and recent detailed experimental analysis [7,8] has shown that significantly higher inlet manifold temperatures and pressures are required to make iso-butane knock than those required for n-butane in a particular test engine at a fixed engine speed and compression ratio.

The third example is given in Fig. 4, in which five different isomeric forms of hexane are shown schematically, along with the related ring compound cyclohexane. Again, the flame temperatures and burning velocities are all nearly the same, while the octane numbers for the six compounds are shown in Table 1.

	Fuel	Octane number
1	n-hexane	25
2	2-methyl pentane	73
3	3-methyl pentane	74
4	2-2 dimethyl butane	92
5	2-3 dimethyl butane	99
6	cyclohexane	80
7	n-butane	92
8	iso-butane	100
9	n-octane	< 0
10	iso-octane	100
11	n-pentane	62
12	n-heptane	0

Table 1. Octane numbers for sample fuels

It is clear that structural factors can have a very large influence on the autoignition properties for these fuels.

Although not illustrated in Figs. 2-4, another factor which can have a comparable influence on autoignition and knock is the absolute size of the fuel molecule. For straight-chain hydrocarbons from n-butane to n-octane, the octane numbers are 92, 62, 25, 0, and less than zero, respectively, with comparable trends for branched-chain paraffins as well.

The kinetic modeling approaches described in this paper show how many of these problems are being addressed at the present time. The important kinetic steps in each temperature regime are discussed in detail, with examples of each type of reaction for a variety of hydrocarbon fuels. Methods are described for identifying the major reaction paths in each temperature regime and for different types of fuel molecules, in those cases where specific experimental kinetic data are not available. Rational techniques for estimating rates of different types of reactions are also discussed.

CONCEPT OF COMPREHENSIVE MECHANISMS

Detailed kinetic models are most often used to simulate experimental results in a single type of experiment, over a very limited range of temperature and pressure. It is often possible to make certain mechanistic simplifications and other assumptions for this type of modeling effort, assumptions which would be valid only for a limited range of operating conditions. However, when the reacting gases follow a complex and extended pressure and temperature history, this type of simplification is no longer possible.

To some extent, any chemical kinetic reaction mechanism is an attempt to simulate the actual reaction history of the reacting gas sample. When these reacting gases encounter a wide range of operating conditions, a great demand is made on the reaction mechanism. Some time ago, Westbrook and Dryer outlined the properties of a so-called "comprehensive" reaction mechanism [13,14], which would be valid over such ranges of operating conditions. The basic idea was that the reaction mechanism should be tested over the entire range of conditions of interest, using experimental

data from a variety of separate experiments under disparate conditions. This means that mechanistic simplifications which are valid only within a limited range of conditions cannot be made.

An additional element essential in the construction of comprehensive reaction mechanisms is that they are built in a definite "stepwise" manner. Mechanisms for complex hydrocarbon fuels are based on previous mechanisms for simpler, smaller fuel molecules. The smallest, most fundamental block in this construction is the reaction mechanism for oxidation of H_2 and CO. The next logical step is the mechanism for CH_2O, followed by those for methane (CH_4) and methanol (CH_3OH), continuing on to successively larger fuels. Comprehensive mechanisms have been developed for a considerable number of hydrocarbon fuels [15-19] as large as n-butane.

The modeling of combustion in an internal combustion engine, and in particular the process of autoignition that leads to engine knock, requires a comprehensive reaction mechanism that is even more general than any which has been developed to date. All of the previous such mechanisms considered combustion problems at temperatures above about 900K, using experimental data from such environments as shock tubes, laminar flames, the turbulent flow reactor, and high temperature stirred reactors. Reactions and products which were important at lower temperatures but which had no importance at 900K and above were therefore not included in these previous models. However, as we will discuss elsewhere in this paper, oxidation processes at lower temperatures, as low as 500K, play an important role in the autoignition and engine knock problem and must be considered. In fact, the dominant reaction steps between 500 and 800 K are distinctly different from those which are important at higher

temperatures and require entirely different elementary reactions and species to be included. Therefore, the reaction mechanisms developed for these problems must be valid for temperatures from 500K to the high temperature ignition levels of 1500K or more. As we will also discuss, the high pressures encountered in engine chambers also add to the constraints placed on the reaction mechanisms to be developed.

Finally, the fuel molecules which we would like to consider in a study of engine knock are considerably larger and structurally more complex than those which have been examined in earlier comprehensive reaction mechanisms. In particular, reaction mechanisms for the ignition of fuels such as n-heptane and iso-octane, the primary reference fuels for knock rating of hydrocarbon fuels in automotive engines, are extremely desireable. The steps required to develop mechanisms for these larger fuels are described below.

Therefore, the present type of modeling approach represents a generalization of the concept of a comprehensive reaction mechanism in that it extends the temperature range of validity to much lower values and to much more complex fuels than were treated previously. This work on development of reaction mechanisms is currently in progress, but the results already obtained have been very instructive and informative.

In the next section, reaction mechanisms for the higher temperature ranges are examined, followed by the complications which begin to appear as the temperature is steadily reduced.

HIGH AND INTERMEDIATE TEMPERATURE IGNITION

Chain Branching Mechanisms

At temperatures in excess of about 1100-1200K, the ignition and combustion of typical hydrocarbon fuels is conceptually quite simple. Following a brief initiation period during which a free radical pool is established, the fuel molecule is systematically broken down into smaller fragments. The principal types of reactions responsible for this fuel consumption process are H atom abstractions from the fuel and other intermediate species, and thermal decomposition reactions of the larger hydrocarbon radicals which are produced. Once the larger fuel and intermediate hydrocarbon species have been converted to CO and H_2, these intermediates are rapidly oxidized to CO_2 and H_2O, releasing a large amount of thermal energy, raising the temperature and pressure of the reacting gas mixture, and effectively completing the overall reaction.

In this high temperature regime, the chain branching features of the combustion reaction mechanism are dominated by the single reaction

$$H + O_2 = O + OH$$

which consumes one H atom and produces two radical species which then accelerate the overall fuel consumption process. This reaction has a fairly high activation energy of about 17 kcal/mole [20], so it requires a high temperature to proceed rapidly. A second reaction

$$H + O_2 + M = HO_2 + M$$

can under some conditions compete effectively with the chain branching reaction, thereby reducing the overall rate of reaction. This recombination reaction is clearly pressure dependent; in addition, its rate has very little temperature dependence. Therefore, as the reacting gas temperature is decreased to about 1000K, or as the pressure is

increased significantly, this second reaction competes for the available H atoms and tends to reduce the overall rate of oxidation.

At temperatures in excess of 1100-1200K, where the $H+O_2 = O+OH$ chain branching reaction is the dominant reaction, the overall rate of reaction and ignition is very fast, compared with the typical residence times in the engine chamber. That is, once the end gas temperatures have reached the point where this high temperature ignition process is important, the attainment of ignition can be considered to be essentially instantaneous. In earlier modeling studies [6,21], we have shown that the autoignition process occurs on a time scale shorter than a millisecond when the gas temperature is greater than 1100K.

When the end gas temperatures fall below about 1100K, the reaction

$$H + O_2 = O + OH$$

becomes much less important than the recombination reaction

$$H + O_2 + M = HO_2 + M \quad .$$

This transition is emphasized by the high pressures (greater than 20 atm) which are encountered in the combustion chamber of a typical automotive engine. As the $H+O_2$ branching reaction becomes less important, another cycle of reactions becomes responsible for the majority of the chain branching which is observed in the engine chamber. This sequence of reactions which leads to chain branching is dominated by

$$\text{fuel} + HO_2 = \text{alkyl} + H_2O_2$$

$$\text{alkyl} + O_2 = \text{olefin} + HO_2$$

$$H_2O_2 + M = OH + OH + M$$

which essentially converts one HO_2 radical to two OH radicals [6]. The HO_2 radical is also regenerated, making this a very efficient chain branching sequence.

This HO_2 sequence requires a sufficiently high temperature to dissociate the H_2O_2 molecule. However, as the temperature increases further, two factors combine to reduce its influence. First, at higher temperatures, the competing reaction

$$H + O_2 = O + OH$$

becomes important. Second, as the temperature increases, the alkyl radicals are consumed primarily by thermal decomposition, often yielding H atoms, as in the examples

$$C_2H_5 + M = C_2H_4 + H + M$$

$$iC_3H_7 = C_3H_6 + H$$

$$HCO + M = H + CO + M$$

$$tC_4H_9 = H + iC_4H_8 \quad .$$

Therefore, there is a fairly narrow range of temperatures over which the temperature is high enough to dissociate H_2O_2 and still low enough that the $H+O_2 = O+OH$ reaction and the alkyl radical decomposition reactions are unimportant.

This temperature regime, where the HO_2-H_2O_2 reactions are most important, is the temperature range in which typical end gases tend to autoignite. Under most practical engine conditions, the end gases ignite at temperatures between 850K and 1100K, exactly the range over which the HO_2-H_2O_2 reactions dominate. Our previous work [6] has shown that antiknock additives such as tetra-ethyl lead (TEL) almost certainly act within this same temperature range by removing HO_2 and/or H_2O_2 from the chain branching reaction sequence through catalytic heterogeneous reactions on the surfaces of solid lead oxide particles.

Detailed Reaction Paths

In this section, we discuss the specific sequences of reactions which consume hydrocarbon fuels at intermediate and high temperature conditions. The first type of reaction is that of the unimolecular decomposition of the fuel molecule itself. This type of reaction is necessary in some situations such as shock tubes and detonations to initiate the overall combustion and provide the first supply of radical species which can then carry out the bulk of the overall combustion process. For relatively large hydrocarbon fuel molecules, such as for C_5 fuels and larger, the decomposition reaction actually consumes an appreciable fraction (i.e. more than 5%) of the fuel. For smaller hydrocarbon fuels, these reactions have been extensively studied, both experimentally and theoretically, the rates of decomposition have been measured and the identities of the product species have been determined. In the case of methane, a C-H bond must be broken, with a bond energy of approximately 104 kcal/mole. For the vast majority of other hydrocarbon fuels, and for all of the fuels which are discussed in the present work, a C-C bond is broken, with a bond energy approximately 10 - 15 kcal/mole less than that for a comparable C-H bond. It is generally observed that when a large fuel molecule decomposes, the products formed are most often as nearly comparable in size as possible. Thus, for n-butane, C_2H_5 + C_2H_5 are the most likely products, rather than nC_3H_7 + CH_3, and the products of iso-butane decomposition are iC_3H_7 + CH_3. Similarly, for n-octane, the most likely products would be $1\text{-}C_4H_9$ + $1\text{-}C_4H_9$ and $1\text{-}C_5H_{11}$ + nC_3H_7. For iso-octane the most probable products are $t\text{-}C_4H_9$ + $i\text{-}C_4H_9$ and $neo\text{-}C_5H_{11}$ + iC_3H_7. These observations, together with the analogous steps for the paraffinic hexanes, are summarized in Table 2.

nC_4H_{10}	= $C_2H_5 + C_2H_5$
iC_4H_{10}	= $nC_3H_7 + CH_3$
nC_8H_{18}	= $nC_4H_9 + pC_4H_9$
iC_8H_{18}	= $tC_4H_9 + iC_4H_9$
nC_6H_{14}	= $pC_3H_7 + nC_3H_7$
2-methyl pentane	= $nC_3H_7 + iC_3H_7$
3-methyl pentane	= $C_2H_5 + sC_4H_9$
2-2 dimethyl butane	= $tC_4H_9 + C_2H_5$
2-3 dimethyl butane	= $iC_3H_7 + iC_3H_7$

Table 2

Products of thermal decomposition reactions of typical fuels

The radical pool is rapidly established after the initiation steps have proceeded to some extent. Once there are a significant number of radical species, the most important reactions are H atom abstractions from the fuel molecules. The most important species which participate in such reactions are OH, O, H, CH_3, HO_2, and other lesser reactants.

The rates of H atom abstraction reactions have been studied in detail for a relatively small number of hydrocarbon fuels. In particular, as the size of the fuel molecule becomes larger, it also becomes important to be able to distinguish between rates of abstraction of H atoms from different bonding sites in the fuel molecule. For example, referring to the two isomeric forms of octane in Fig. 2, all of the H atoms indicated by the numeral '1' in n-octane are bonded to primary sites, while those indicated

by 2, 3, and 4 are bonded to secondary sites. The primary H atoms are more firmly bonded to the molecule and therefore require a greater amount of energy for them to be removed. The binding energies of all of the secondary H atoms are very nearly the same in n-octane, but it is still necessary to account separately for each logically distinguishable H atom site in the molecule because the subsequent history of each of the products may be different, as we will show below. The same type of distinctions can be seen in the case of iso-octane in Fig. 2. The H atoms indicated by the letter 'a' are all logically equivalent, bonded at primary sites to the methyl groups at one end of the molecule. Those marked 'd' are also bound to primary sites, but they are located at the other end of the molecule; removal of an 'a' H atom will lead to different products than abstraction of a 'd' H atom. The H atoms marked by a 'b' are attached to secondary sites, and the H atom marked by 'c' is at a tertiary site, where it is the most weakly bound H atom in iso-octane.

The reactions of the product alkyl radicals generally consist of either a unimolecular decomposition reaction or a reaction with molecular oxygen. At intermediate and high temperatures the decompostion reaction tends to dominate. A considerable body of modeling and theoretical literature in recent years [14,22] has demonstrated that the thermal decomposition steps can be predicted very well by using the principle of β-scission. Of primary importance in predicting the overall reaction rate for a given fuel in this temperature regime is the nature of the products of these alkyl radical decomposition reactions. Those reaction steps which lead to H atoms generally lead to an accelerated rate of reaction, since the H atoms then react by

$$H + O_2 = O + OH$$

and lead to chain branching, while reaction paths which lead to more stable products, particularly methyl radicals, generally lead to a much slower overall rate of reaction. Reactions of alkyl radicals with O_2 at intermediate and high temperatures generally lead to a reduced rate of reaction since the HO_2 radicals are less reactive than the H atoms produced by alkyl radical decomposition reactions.

The significance of the differently labeled H atoms in Fig. 2 can then be shown by determining which H atom abstraction reactions lead eventually to H atom production and which do not. In the case of n-octane, if we indicate by 1-C_8H_{17} that alkyl radical which results when the '1' H atom is abstracted, and similarly for 2-C_8H_{17}, 3-C_8H_{17} and 4-C_8H_{17}, then the principle of β-scission predicts the following families of decomposition products:

$$1\text{-}C_8H_{17} = C_2H_4 + C_2H_4 + C_2H_4 + C_2H_4 + H$$

$$2\text{-}C_8H_{17} = C_3H_6 + C_2H_4 + C_2H_4 + CH_3$$

$$3\text{-}C_8H_{17} = {}_1C_4H_8 + C_2H_4 + C_2H_4 + H$$

$$4\text{-}C_8H_{17} = {}_1C_5H_{10} + C_2H_4 + CH_3 \quad .$$

Therefore production of H atoms and subsequent chain branching result from the abstraction of the '1' and '3' H atoms from n-octane, while abstraction of the '2' and '4' H atoms leads to production of stable olefins and relatively unreactive methyl radicals, which slow the overall rate of reaction.

The same type of analysis is straightforwardly applied to the other fuels indicated in Table I. In particular, for iso-octane, using the same type of alkyl radical definition as that used for n-octane in Fig. 2:

$$\dot{a}\text{-}C_8H_{17} = iC_4H_8 + C_3H_6 + CH_3$$

$$b\text{-}C_8H_{17} = C_7H_{14} + CH_3$$

$$\dot{c}\text{-}C_8H_{17} = iC_4H_8 + iC_4H_8 + H$$

$$d\text{-}C_8H_{17} = iC_4H_8 + C_3H_6 + CH_3$$

where two structurally different heptene molecules are possible. In this case, only the abstraction of the tertiary H atom in iso-octane leads to the production of H atoms and high temperature chain branching; all of the other 17 H atom sites lead to production of stable intermediates and methyl radicals. As a result of this type of analysis, it is clear that the high temperature ignition of n-octane should be much more rapid than that of iso-octane.

This type of modeling analysis has been applied recently to ignition of large fuels behind shock waves [23-25] and for high temperature well-stirred reactors [26], where the high temperature reaction mechanism is of primary importance. All of the initiation and fuel composition reactions already described above occur at high rates and determine the overall rate of reaction. This overall analysis has been greatly simplified, emphasizing only the most dominant features of the high and intermediate temperature kinetics mechanisms. Many additional features can play significant roles, and these further details are discussed in detail in a number of previous publications [14,27,28].

In many cases, the rate of high temperature ignition correlates well with the octane number. For example, the octane number of iso-octane, which we have seen ignites very slowly at high temperatures, has the very high octane number of 100, while the octane number for n-octane is very low, actually less than zero. There are many other examples of this type of overall correlation between the rate of high temperature and the octane

number. However, there are also a large number of cases in which this agreement breaks down. As an example of this type of problem, we can consider the cases of neopentane and 2-2-dimethyl butane. The structures of these fuels are summarized in Fig. 5. If we follow the product distributions of the alkyl radical decomposition reactions, it is clear that all twelve of the H atom abstraction possibilities in neopentane lead to methyl radicals and iso-butane. Therefore the high temperature ignition of this fuel should be very slow. Furthermore, the knock resistance and octane number of neopentane are very high, with an octane rating of 90. The second fuel shown in Fig. 5 is 2-2-dimethyl butane, which is really equivalent to neopentane with a methyl group replaced by an ethyl radical. Of its 14 H atoms, abstraction of 12 of them leads to H atom production and high temperature chain branching. As a result, the high temperature ignition of this fuel would be expected to be very rapid. However, the octane number of this fuel is very high, with a value of 97, even higher than the value of 90 observed for neopentane.

There are many other examples of this lack of correlation between the rate of H atom production and high temperature ignition rate with the octane number. The immediate conclusion is that the octane number and knock susceptibility are not determined by the high temperature reaction mechanisms alone. In the next section, the chemical reactions which control the rate of combustion at lower temperatures will be described.

EXTENSIONS TO LOW TEMPERATURE

Below temperatures of about 800 K, alkyl radicals produced by H atom abstraction reactions from the fuel molecule thermally decompose at a relatively slow rate. These radicals instead react with O_2 to produce alkylperoxy radicals which then react in a variety of ways:

$$R + O_2 = RO_2^* = \text{olefin} + HO_2$$
$$= RO_2$$
$$= R + O_2$$

The simplest result of such reactions is the production of an olefin species and HO_2 radicals. The detailed mechanism of this process has been investigated in depth by Slagle et. al. [29] and Baldwin and Walker [30]. The alkyl peroxy radical, RO_2, can also react with the fuel or can undergo an internal H-atom abstraction, both of which lead to the formation of hydroperoxides, ROOH and QOOH,

$$RO_2 + R'H = R' + ROOH$$

or $$RO_2 = QOOH$$

where R'H is the fuel, and the species Q is the radical species R minus one H atom. Both hydroperoxides can decompose to form OH radicals,

$$ROOH = RO + OH$$

$$QOOH = \text{O-heterocycle} + OH$$

but ROOH produces two radicals and QOOH produces only one radical. The hydroperoxide radical QOOH can also undergo further reaction with molecular oxygen and yield two OH radicals and the radical Q'O,

$$QOOH + O_2 = O_2QOOH$$

$$O_2QOOH = \text{aldehyde} + Q'O + OH + OH \quad .$$

In summary, if the alkyl radical R eventually produces the alkyl hydroperoxide ROOH, three radicals, R', RO and OH, are produced and one R radical is consumed. The amount of radical multiplication for this reaction sequence is a factor of 3. If the R radical follows the path of the hydroperoxide radical QOOH, either one OH radical is produced or three radicals (Q'O, OH, and OH) are produced. The amount of radical multiplication for this reaction sequence is either 1 or 3, respectively.

All the above reaction sequences produce an abundant amount of OH radicals. Production of OH radicals is a key feature of the low temperature kinetic mechanism since OH predominantly then reacts with the fuel, producing water and releasing a significant amount of heat:

$$RH + OH = R + H_2O + 23 \text{ kcal/mole} \quad .$$

This heat release increases the temperature of the end gas. As discussed in a previous section, a small amount of heat release at low temperatures will cause the end gas to achieve high temperature ignition at an earlier time in the cycle (Fig. 1). If the end gas autoignites before it is consumed by the flame, engine knock will result.

For alkyl peroxy radicals (RO_2) which have about four or more carbon atoms, the path involving an internal H-atom abstraction is dominant [30]. We will now describe specifically how we have treated these reaction paths and estimated their reaction rates.

Internal H-atom abstractions occur by the formation of a ring-like transition state. Different types of internal H-atom transfers are identified by the number of carbon and oxygen atoms in the ring-like

structure. The letters p, s, and t for primary, secondary and tertiary, respectively, signify the type of H-atom transferred [31]. An example of a 1,5p H-atom transfer in a s-butyl peroxy radical is:

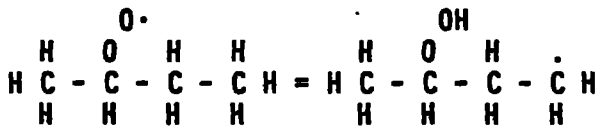

Rates for internal H-atom transfer depend on the number of atoms in ring-like transition state, the type of H-atom being abstracted, and the number of H-atoms that are accessible for abstraction. Baldwin, Walker and coworkers [31,32] have estimated reaction rates for most of the important types of internal H-atom abstractions. They determined rates at 753 K and estimated activation energies. A tabulation of their rate information is given in Table 3 where the reaction rate expressions are the rate per H-atom abstracted. To obtain the rate for a given molecule, the frequency factor A needs to be multiplied by the number of possible H-atoms that can be abstracted for a type of particular ring. For example, if one is considering a 1,4p H-atom abstraction and there are 3 primary H-atoms that can be abstracted for this ring size, one would multiply the rate given in Table 3 by a factor of 3. To determine the reaction rates in Table 3 from their experimental data, Baldwin and Walker required the value of the equilibrium constant for the addition reaction of O_2 to the alkyl radical. We have recalculated the rates for the internal H-atom abstractions using more recent values for this equilibrium constant. Slagle and Gutman [33] have recently measured the equilibrium constant for

$$iC_3H_7 + O_2 = iC_3H_7O_2 \quad .$$

We have employed their measured value to estimate the equilibrium constant for $R+O_2=RO_2$ when R is a secondary or primary radical. The equilibrium constants used by Baldwin and Walker were calculated using Benson's

additivity rules [34]. The use of Slagle and Gutman's value for this equilibrium constant decreased the isomerization rates given in Table 3 by approximately an order of magnitude from those originally reported by Baldwin and Walker. For the case of a tertiary alkyl radical, the equilibrium constant estimated by Morgan et al. [35] for t-butyl radicals was employed.

In the following discussion, we address the specific case of RO_2 radicals formed from iso-octane and their internal H-atom abstractions. Iso-octane is a particularly instructive case, since it exhibits most of the possible types of internal H-atom abstractions. We will estimate the reaction rates and examine reaction paths of the RO_2 radicals and subsequent products for this case.

Table 4 lists the possible types of internal H-atom abstractions from the iso-octyl peroxy radicals. The types of alkyl peroxy radicals formed from iso-octane are denoted in the same manner as the alkyl radicals shown in Fig. 2. The suffix a, b, c, or d indicates the site where molecular oxygen has added to the alkyl radical. The last column in Table 4 lists the identity of the O-heterocyclic compounds, QO, that result from the decomposition of QOOH and the relative rates at which each of the O-heterocyclic compounds would be expected to be formed. These rates were calculated to predict the relative production rates of each type of oxygenate.

The relative rates of formation of the O-heterocyclic compounds, QO, were estimated as follows. During the oxidation of iso-octane, most of the parent alkyl radicals are produced from H-atom abstraction from the fuel by OH. The relative amount of alkyl radical, R, is approximately determined by the relative rates of the reactions:

$$i\text{-}C_8H_{18} + OH = aC_8H_{17} + H_2O$$

$$i\text{-}C_8H_{18} + OH = bC_8H_{17} + H_2O$$

$$i\text{-}C_8H_{18} + OH = cC_8H_{17} + H_2O$$

$$i\text{-}C_8H_{18} + OH = dC_8H_{17} + H_2O$$

We employed primary, secondary and tertiary H-atom abstraction rates estimated from the measurements work of Tully and coworkers [36,37]. The amount of RO_2 can be calculated from the equilibrium constant K_{eq} of $R+O_2=RO_2$

$$[RO_2] = K_{eq}[O_2][R]$$

where K_{eq} is in concentration units. For the cases in which R is a primary or secondary iso-octyl radical, we used measured values of K_{eq} from Slagle et al. [33]. When R is a tertiary radical, we used a calculated value of K_{eq} from Morgan et al. [35]. We estimated the relative amounts of RO_2 at 800 K since this is the approximate temperature where significant fuel consumption started for n-butane oxidation under engine conditions [8]. At 800 K, a typical oxygen concentration under engine conditions is 2.5×10^{-5} moles/cm^3. The normalized amounts of RO_2 calculated from the above relation are given in Table 4 under "fraction". We then calculated the rate of production of each O-heterocycle by obtaining the product of the H-atom isomerization rate (Table 3), the number of accessible H-atom sites, and the relative fraction of RO_2 in Table 4.

The calculated rates in Table 4 can be used to predict the predominant O-heterocyclic compounds for iso-octane oxidation under engine conditions. The compound predicted to be in the highest concentration, significantly higher than any of the others listed in Table 4, is 2,2,4,4-tetramethyl-hydrofuran. This is also the most prevalent O-heterocycle measured by Barnard and Harwood [38] in their study of

iso-octane oxidation at 620 K. This product is a result of the 1,6t internal H-atom abstraction (Fig. 6, Reaction 7). From Table 4, the O-heterocycles present in the the next highest concentration are the oxirans, which are about a factor of 10 below 2,2,4,4-tetramethyl-hydrofuran. Barnard and Harwood did not report the concentrations of any oxirans, but they claimed they were, at most, minor products. Following the oxirans, the next highest rates in Table 4 are for the formation of 2-t-butyl-3-methyl-oxetan and 2,2-dimethyl-3-isopropyl oxetan. Of the possible C_8 O-heterocycles, Barnard and Harwood observed these two products in the next highest concentration after 2,2,4,4-tetramethyl hydrofuran. Consequently, the method outlined here gives reasonable estimates for the relative amounts of O-heterocycles in iso-octane oxidation.

Another feature of the results in Table 4 is that they predict that O-heterocycles formed from the dC_8H_{18} radical will be present in only minor concentrations. Similar results have been found for other alkyl peroxy radicals with the O_2 in the tertiary position. Baldwin and coworkers [31,39] reported analogous trends for the t-$C_4H_9O_2$ radical where they observed only small amounts of oxygenates resulting from internal H-atom abstractions of this radical. The explanation of the low yields of O-heterocycles from the t-alkyl peroxy radical (t-RO_2) is probably due to its low ceiling temperature. The ceiling temperature is defined as the temperature where $[RO_2]/[R] = 1$ at a given O_2 concentration [40]. From the equilibrium constant K_{eq} of the addition reaction of molecular oxygen to the alkyl radical, the ceiling temperature occurs when $K_{eq}[O_2] = 1$. At a O_2 partial pressure of 0.1 atm, the ceiling temperature for t-RO_2 is about 709 K (see [35]), while that for primary RO_2 and secondary RO_2 is about 847 K (see [33]). Consequently,

t-RO_2 falls apart at a significantly lower temperature than the primary or secondary RO_2, and it is present in much lower concentrations as seen by the relative concentrations in Table 4. This low concentration of t-RO_2 radicals leads to low rates of internal H-atom abstractions and oxygenate production.

Another important issue concerning internal H-atom abstractions is the specific fate of the QOOH hydroperoxide. There are two possible paths. The first path is the decomposition of QOOH. This reaction path gives one OH radical for each original alkyl radical, R, consumed and does not provide any radical multiplication which would explain the rapid oxidation rate of hydrocarbons at low temperatures. The alternative consumption path for QOOH consumption is further addition of molecular oxygen to QOOH. This reaction sequence gives three radicals for each original alkyl radical consumed and provides rapid radical production.

The reaction path when O_2 adds to QOOH in the case of the $aC_{18}H_{17}$ radical is shown in Fig. 6. This reaction path is analogous with a similar path suggested by Benson [41] for n-alkanes. The key feature of this reaction sequence is that three radicals (including two reactive OH radicals) are produced for each $aC_{18}H_{17}$ consumed, providing a significant amount of radical multiplication. These OH radicals rapidly react with the fuel to yield water and a large amount of heat release. The heat release raises the temperature of the mixture and increases the reaction rate. In summary, the above radical multiplication combined with heat release causes the oxidation process to proceed more rapidly toward autoignition.

Table 3
Rates of Alkyl Peroxy Isomerization Reactions

Type of H-Transfer	Reaction Rate log A	E_a	log k at 800 K
1,4p	10.98	30.0	2.8
1,5p	10.61	27.0	3.2
1,6p	10.24	25.1	3.4
1,4s	10.88	26.5	3.6
1,5s	10.79	23.4	4.4
1,6s	11.00	21.5	5.1
1,4t	11.33	23.0	5.0
1,5t	11.00	20.1	5.5
1,6t	11.00	17.9	6.1

Table 4

Internal H-Atom Abstractions for Iso-Octane

type of alkyl peroxy radical	fraction	type of abstraction	No. of C-H sites	total rate	product, QO
a$C_8H_{17}O_2$	0.44	1,5p	6	1.1×10^4	2-2-methylbutyl-1-oxetan
		1,5s	2	5.8×10^4	2,2-dimethyl-3-isopropyl-oxetan
		1,6t	1	1.5×10^6	2,2,4,4-tetramethyl-hydrofuran
		1,7p	6	2.0×10^4	2,2,5-trimethyl-tetrahydropyran
b$C_8H_{17}O_2$	0.29	1,4t	1	1.2×10^5	2-methyl-2-neopentyl-oxiran
		1,5p	3	5.6×10^3	3-neopentyl-oxetan
		1,5s	2	5.8×10^4	2-t-butyl-3-methyl-oxetan
		1,7p	9	2.9×10^4	2,2,5-trimethyl-tetrahydropyran
c$C_8H_{17}O_2$	0.27	1,4t	1	1.2×10^5	2,2-dimethyl-3-tertbutyl-oxiran
		1,5p	6	1.1×10^4	2-t-butyl-3-methyl-oxetan
		1,5p	9	1.6×10^4	2,2-dimethyl-3-isopropyl-oxetan
d$C_8H_{17}O_2$	0.0035	1,4p	6	9.5×10^1	2-methyl-2-neopentyl-oxiran
		1,4s	2	2.0×10^2	2,2-dimethyl-3-tertbutyl-oxiran
		1,6p	9	6.3×10^2	2,2,4,4-tetramethyl-hydrofuran

EXAMPLES OF MODEL TESTS IN DIFFERENT ENVIRONMENTS

Before a kinetic model can be applied to a practical problem like that of engine knock, it must first be validated through a series of numerical tests against experimental data obtained in somewhat more idealized conditions. In most cases, any one of these experiments will cover a rather limited range of operating conditions. However, the given experiment will generally provide a rather demanding test of the reaction mechanism under those limited conditions. In order to "pass" the test, the reaction mechanism must accurately reproduce the observed experimental results under each of the sets of available conditions. Only when the reaction mechanism has passed such tests under an entire range of conditions which spans those of concern in the practical problem can the model be expected to provide realistic and reliable predictions for the practical, applied problem such as the end gas autoignition in an engine chamber.

In this section, we will very briefly review the types of experimental studies which provide valuable tests for the reaction mechanisms which are being developed to study hydrocarbon autoignition.

Shock Tubes

Shock tube experiments are an excellent test of the high temperature reaction mechanism for hydrocarbon oxidation [13,14]. The nearly instantaneous attainment of high temperature (i.e. > 1200K) and fairly high pressure (i.e. > 3 atm) means that the results are completely independent of the low and intermediate temperature regime reaction subsets. The most common observable quantity in such experiments is the ignition delay time; species concentration variations with time and other

possible diagnostics are rather uncommon in such experiments, so the most common reaction mechanism test is an integral test of the total ignition delay period.

In a series of shock tube experiments, Burcat et al. [42] used mixtures of n-alkanes, oxygen, and argon in proportions which were intended to simulate fuel-air conditions. The ratio of argon to oxygen was 5:1 rather than the very high value which is typical of many shock tube experiments. This means that the total heat release and temperature increase resulting from the ignition will be substantial. In the experimental paper, the n-alkanes from C_1 to C_5 were considered; the results were presented in terms of the observed ignition delay time. Methane was found to be anomalously slow to ignite, while all of the other n-alkanes were very similar in their rate of ignition, with ethane being slightly faster to ignite than the C_3 - C_5 fuels. In an earlier paper [25], computer modeling results were compared with the experimental results, with the overall performance of the numerical model being quite satisfactory. These results are summarized in Figure 7, with the results for ethane not shown, but with computed results for iso-butane included. Following the chain branching arguments presented earlier in this paper, ethane reacts most rapidly because virtually all H abstraction reactions lead to ethyl radicals and H atoms, which accelerate the rate of ignition. Propane, n-butane and n-pentane produce a mixture of methyl radicals and H atoms, and their ignition delay periods are all very similar.

A later study examined the shock tube ignition of mixtures of n-octane, n-heptane, and iso-octane with oxygen and argon, again with the

ratio of argon to oxygen equal to 5:1 and the ratio of fuel to oxygen equal to the stoichiometric value [24]. Ignition delays were computed at initial temperatures from 1250 K to 1500 K, with the initial density equal to a constant value of 3.54×10^{-3} gm/cm^3, as used in previous studies [24,25,43]. The results for the large hydrocarbon fuels are summarized in Figure 8, in which some of the smaller n-alkane results are included as well. It is clear that the ignition delay times for both of the straight-chain fuels n-octane and n-heptane are shorter than those for the C_1 - C_5 n-alkanes, and that there is only a very small difference between n-heptane and n-octane. Furthermore, iso-octane is significantly slower to ignite than the straight-chain fuels over the entire temperature range of interest.

In the high temperature regime, at pressures less than 10 atm (1 MPa), the kinetic analysis already presented in terms of H atoms, methyl radicals, intermediate olefins, and their relative rates of production, provides a rather simple, straightforward, uncomplicated picture of hydrocarbon fuel ignition. The straight-chain fuels produce relatively large amounts of H atoms through alkyl fragmentation into ethyl radicals. These H atoms provide large rates of chain branching and rapid rates of fuel ignition. In strong contrast, the branched-chain iso-octane results in very few H atoms and a very low rate of chain branching and a correspondingly low rate of ignition.

Flow Reactors

The turbulent flow reactor provides an experimental environment which is complementary to that of the shock tube and very useful for carrying out development of detailed chemical kinetic models. The temperatures are considerably lower than those of the shock tube and fall in exactly the same range (900 - 1200K) in which the reaction mechanism undergoes the transition from HO_2-dominated chain branching to that dominated by the $H+O_2 = O+OH$ reaction. In contrast to the shock tube, initiation reactions play virtually no part in the flow reactor, but the important period of fuel consumption and production of stable intermediates is easily accessible in the flow reactor.

The most prominent experimental program in recent years devoted to exploring hydrocarbon kinetics in the flow reactor has been that at Princeton University. The experimental facility is described by Dryer and Glassman [44], although considerable further development of the experimental capabilities has been carried out since the time of that paper. Detailed results from this facility have been used in a large number of studies in recent years [15-18,23,45] to develop the understanding of intermediate and high temperature kinetic processes which control hydrocarbon combustion.

The turbulent flow reactor can study temperatures as low as approximately 900K. As the temperature is further reduced, the overall rate of fuel conversion becomes quite small, and the extent of reaction within the test section of the reactor becomes too low to be able to detect the changes in composition. It is then necessary to switch to an experimental configuration which is better suited to following the much longer time scales of the hydrocarbon oxidation process.

Low Temperature Reactors

Three types of experimental facilities are generally most useful to study oxidation at temperatures between about 500 and 900K. These are the static reactor, the continuously stirred tank reactor (cstr), and the rapid compression machine. Historically, the static reactor has been most prominent for many years, and perhaps thousands of experimental studies in static reactors have been carried out to provide a wealth of data and insight into oxidation kinetics. From the point of view of kinetic mechanism development, these experiments have been essential in terms of qualititative information; from a quantitative aspect, modeling these experiments is often difficult because of the influence of the walls, both due to their kinetic activity and to the fact that heat transfer through the walls to the outside is difficult to quantify. Recent contributions to the kinetic mechanism development described in this paper have been provided by static reactor experiments carried out by Kaiser [46] and Wilk et al. [47,48].

The cstr is a more recent development, described in detail by Griffiths [49] and Lignola [50]. This system is a flowing one in which a reaction chamber has fresh reactants flowing into it, reaction is taking place in the reactor, and reaction products are flowing out of the chamber. The contents of the reactor are well stirred, so spatial homogeneity is maintained in the reactor. As a result, the system approaches the ideal conditions where there is a single reaction zone with steady flow in and out of that zone. Such a system is quite simple to simulate numerically, and an important advantage of both the model and the experiment is that more complex classes of behavior can be studied than those accessible in the static reactor (e.g. [51]), including periodic cool flames, periodic ignition, and a wealth of other periodic behavior.

The rapid compression machine has been valuable for reaction kinetics development in several ways. A vast number of these experiments were used to develop and test the Shell Model [1-5] discussed above. These experiments have been used extensively by Griffiths et al. (e.g. [52,53]) to study hydrocarbon fuel oxidation, especially in the negative temperature coefficient region, kinetic information which is essential in developing kinetic models for the lower temperature regime. A further advantage of the rapid compression machine data is that, in addition to the temperature range of the experiments, the pressures attained are significantly higher than those commonly found in static reactors and the cstr and therefore much closer to those encountered in knocking engines. Experimental data from the rapid compression machine will play an increasingly important role in future mechanism development.

Knocking Engine

Experimental and modeling investigations into actual engines allow one to address the entire temperature history of the end-gas from 400 K to burnt gas temperatures. Both temperature and species concentration histories of the end gas can be measured. Green and coworkers [7-9] have experimentally investigated engine knock in the Sandia optical research engine, measuring autoignition times of hydrocarbon-air mixtures, primarily with n-butane and iso-butane as fuels. In addition, gas sampling techniques were used to determine species concentration histories in the end gas.

We have numerically simulated the series of engine cycles that were experimentally investigated by Green and coworkers. The model assumed that the only way in which the end gas interacted with the remainder of the combustion chamber is through the compressional work done on the end gases by the moving piston and, when spark ignition occurs, by the flame front. Transport processes in the end gases were neglected.

The calculations were begun at a time of 120° before TDC, the time at which the first temperature and experimental pressure measurements were available. It is unlikely that a significant amount of reaction occured prior to this time in the experiment because of the low temperature (less than 550 K). The initial composition of the end gases consisted of a stoichiometric mixture of fuel and air.

Throughout the computations, the measured end-gas pressure history is followed. However, the end-gas temperature history determined using the thermodynamic analysis is imposed only until the calculation indicates that heat release due to chemical reaction in the end gas has become

significant. The end-gas temperature is then computed directly by the kinetics model, thus including the effects of heat release in the end gas. The advantage of this approach is that it allows us to include as much engine operating data as possible in the model. Processes such as flame propagation in the other parts of the engine chamber, piston motion, and heat transfer to the engine walls can be incorporated. On the other hand, if significant heat release occurs due to reactions not included in the kinetic model, then this heat release is unaccounted for in the numerical simulation. The observation that the kinetic model nearly reproduces the measured species concentrations provides some evidence that we have included all the important reactions paths.

The autoignition times predicted by the model are compared to the measured times of Green and coworkers in Table 5. Results are given for both for iso-butane and n-butane and for a range of engine speeds and intake manifold temperatures. The predicted times closely match the measured times, except for the lowest engine speed.

Again referring to Fig. 1, the agreement between computed and experimentally observed times of autoignition at nearly all engine speeds indicates that the heat release is computed adequately over the entire range of temperatures experienced by the end gas. The disagreement at the lowest engine speeds, where the time spent in the lowest temperature range is proportionally the greatest, indicates that the low temperature heat release mechanisms are not yet sufficiently well treated by the model and must be improved. Work in this area is continuing.

In an earlier discussion, the point was made, based on previous modeling studies [6], that the addition of tetraethyl lead inhibits the chain reaction in the 800-1000K temperature range by removing HO_2 and

H_2O_2 from the reaction pool. Therefore the end gases must achieve a higher temperature before the chain reaction can proceed to autoignition. Schematically, this is illustrated in Fig. 1, showing how autoignition of the more reactive case given by the dashed curve can be retarded until a higher temperature T_2 is reached. If, during the time interval between the arrival of this curve at T_1 and T_2 is sufficient for the flame to consume the remaining end gas, then this inhibition of the intermediate-to-high temperature ignition can be said to have accomplished an antiknock function.

SUMMARY

We can use Fig. 1 to provide an overview of the material presented above on the chemical kinetic factors affecting engine knock and autoignition. The primary point is that the reaction history in general, and the heat release rates in particular, must be followed for the end gas in an engine combustion chamber over the entire range of temperatures encountered. Even though the rates of reaction and heat release are relatively low at temperatures below about 700K, they can still influence the time at which autoignition occurs. This is possible because the end gas temperature at which autoignition is observed is a weak function of engine operating conditions. Fuels which have more heat release at lower temperatures (i.e. the dashed curve in Fig. 1) but have roughly the same autoignition temperature as fuels which do not release significant amounts of heat at lower temperatures (the solid curve in Fig. 1) will reach this ignition temperature at significantly earlier times and will therefore be more likely to knock.

The tendency to knock can be modified by changes in the value of the ignition temperature as well as by changes in the amount of low temperature heat release. We have seen how the addition of TEL effectively raises the ignition temperature, thereby increasing the knock rating of the fuel-additive mixture. Knock ratings of fuels with significantly different autoignition temperatures will similarly be different, and this will affect the knock ratings of blends of fuels.

Therefore, the tendency of a given fuel to knock can be influenced both by its degree of low temperature heat release (its cool flame activity) and by the value of its ignition temperature. Thus iso-octane has a much higher octane number than n-heptane because its cool flame activity is much lower and because its high temperature ignition temperature is somewhat higher. The knock tendency of a given fuel can therefore be altered by changing either the low temperature heat release or the ignition temperature, or by changing both parameters, through the use of blending fuels or by using additives.

We have shown how all these processes are kinetically controlled to a considerable extent. It is not possible to provide a truly predictive numerical model of the end gas chemistry and engine knock for arbitrary fuels, additives, fuel mixtures, and generalized engine operating conditions without including in detail the chemical kinetic processes which are controlling the observed behavior. Although considerable progress has been made in this area, as illustrated in the earlier sections of this paper, this work is only beginning, and a great deal of further model and kinetic mechanism development remains to be done.

Table 5

Predicted and Measured Autoignition Times

Fuel	RPM	Manifold Temp [°C]	$\tau_{measured}$ [ms]	$\tau_{predicted}$ [ms]
iso-butane:				
	300	219	-1.27	0.17
	600	217	1.70	1.61
	900	219	1.89	1.78
	600	194	1.78	1.76
	600	170	1.95	1.98
	600	157	2.23	2.23
n-butane:				
	300	162	1.3	1.57
	600	155	2.8	2.85

ACKNOWLEDGMENTS

We have benefited greatly from extensive discussions, collaborative interactions, and constructive criticisms from a large number of colleagues. In particular, we appreciate the considerable contributions of E. I. Axelsson, K. Brezinsky, N. P. Cernansky, F. L. Dryer, R. M. Green, J. Warnatz, and R. D. Wilk. This work was supported by the U. S. Department of Energy, Division of Energy Conversion and Utilization Technologies and the Office of Basic Energy Sciences, Division of Chemical Sciences. THis work was carried out under the auspices of the U. S. Department of Energy by the Lawrence Livermore National Laboratory under contract NO. W-7405-Eng-48.

References

1. Halstead, M.P., Kirsh, L.J. and Quinn, C.P., "The Autoignition of Hydrocarbon Fuels at High Temperatures and Pressures - Fitting of a Mathematical Model", Combust. Flame 30, 45 (1977).

2. Cox, R.A., and Cole, J.A., Combust. Flame 60, 109 (1985).

3. Kirsch, L.J., and Quinn, C.P., "Progress Towards a Comprehensive Model of Hydrocarbon Autoignition", J. Chim. Phys. 82, xxx (1985).

4. Natarajan, B. and Bracco, F.V., "On Modeling Auto-Ignition in Spark-Ignition Engines", Combust. Flame 57, 179 (1984).

5. Hu, H.,and Keck, J.C., "Autoignition of Adiabatically Compressed Combustible Gas Mixtures", SAE paper SAE-87xxxx (1987).

6. Pitz, W.J., and Westbrook, C.K., "Chemical Kinetics of the High Pressure Oxidation of n-Butane and Its Relation to Engine Knock", Combust. Flame 63, 113 (1986).

7. Cernansky, N.P., Green, R.M., Pitz, W.J., and Westbrook, C.K., "Chemistry of Fuel Oxidation Preceding End-Gas Autoignition", Combust. Sci. Technol. 50, 3 (1986).

8. Green, R.M., Parker, C.D., Pitz, W.J., and Westbrook, C.K., "The Autoignition of Isobutane in a Knocking Engine", Society of Automotive Engineers paper SAE-870169 (1987).

9. Smith, J. R., Green, R. M., Westbrook, C. K., and Pitz, W. J., "An Experimental and Modeling Study of Engine Knock", Twentieth Symposium (International) on Combustion, p. 91, The Combustion Institute, Pittsburgh (1984).

10. Gluckstein, M.E., and Walcutt, C., "End-Gas Temperature-Pressure Histories and their Relation to Knock", SAE Trans. 69, 529 (1961).

11. Obert, E.F., Internal Combustion Engines and Air Pollution, Harper and Row, Publishers, Inc., New York, 1973, p.234-235.

12. "Knocking Characteristics of Pure Hydrocarbons", American Society For Testing Materials, ASTM Special Publication No. 225, 1958.

13. Westbrook, C. K., and Dryer, F. L., "Chemical Kinetics and Modeling of Combustion Processes", Eighteenth Symposium (International) on Combustion, p. 749, The Combustion Institute, Pittsburgh (1981).

14. Westbrook, C.K., and Dryer, F.L., "Chemical Kinetics of Hydrocarbon Combustion", Prog. Energy Combust. Science 10, 1 (1984).

15. Westbrook, C. K., and Dryer, F. L., "A Comprehensive Mechanism for Methanol Oxidation", Combust. Sci. Technol. 20, 125 (1979).

16. Westbrook, C. K., Dryer, F. L., and Schug, K. P., "A Comprehensive Mechanism for the Pyrolysis and Oxidation of Ethylene", Nineteenth Symposium (International) on Combustion, p. 153, The Combustion Institute, Pittsburgh (1983).

17. Westbrook, C. K., and Pitz, W. J., "A Comprehensive Chemical Kinetic Reaction Mechanism for Oxidation and Pyrolysis of Propane and Propene", Combust. Sci. Technol. 37, 117 (1984).

18. Pitz, W. J., Westbrook, C. K., Proscia, W. M., and Dryer, F. L., "A Comprehensive Chemical Kinetic Reaction Mechanism for the Oxidation of n-Butane", Twentieth Symposium (International) on Combustion, p. 831, The Combustion Institute, Pittsburgh (1985).

19. Miller, J.A., Mitchell, R.E., Smooke, M.D., and Kee, R.J., "Toward a Comprehensive Chemical Kinetic Mechanism for the Oxidation of Acetylene: Comparison of Model Predictions with Results from Flame and Shock Tube Experiments", Nineteenth Symposium (International) on Combustion, p. 181, The Combustion Institute, Pittsburgh (1983).

20. Baulch, D. L., Drysdale, D. D., Horne, D. G., and Lloyd, A. C., Evaluated Kinetic Data for High Temperature Reactions, vols. 1 and 2, Butterworths, London, 1973.

21. Pitz, W.J., and Westbrook, C.K., "Interactions between a Laminar Flame and End Gas Autoignition", Prog. Astro. and Aero. 105, 293, (1986).

22. Dryer, F. L., and Glassman, I., "Combustion chemistry of chain hydrocarbons", Alternative Hydrocarbon Fuels; Combustion and Chemical Kinetics, C. T. Bowman and J. Birkeland, eds., vol. 62, Prog. Astr. Aeronaut. (1978).

23. Axelsson, E. I., Brezinsky, K., Dryer, F. L., Pitz, W. J., and Westbrook, C. K., "Chemical Kinetic Modeling of the Oxidation of Large Alkane Fuels: N-Octane and Iso-Octane", Twenty First Symposium (International) on Combustion, in press (1987).

24. Westbrook, C.K., and Pitz, W.J., "Kinetic Modeling of Autoignition of Higher Hydrocarbons -- n-Heptane, n-Octane, and iso-Octane", proceedings of the 2nd Workshop on Modelling of Chemical Reaction Systems at the Universität Heidelberg, Heidelberg, W. Germany, 11-15 August 1985.

25. Westbrook, C.K., and Pitz, W.J., "Chemical Kinetics of the Influence of Molecular Structure on Shock Tube Ignition Delay", in Shock Waves and Shock Tubes (D. Bershader and R. Hanson, Eds., Standford University Press, Stanford, CA), p.287, 1986.

26. Westbrook, C.K., Pitz, W.J., Thornton, M.M., and Malte, P.C., "A Kinetic Modeling Study of N-Pentane Oxidation in a Well-Stirred Reactor", submitted for publication, 1987.

27. Westbrook, C.K., "Chemical Kinetic Modeling of Higher Hydrocarbon Fuels", AIAA J. 24, 2002 (1986).

28. Westbrook, C.K., "Numerical Simulation of Chemical Kinetics of Combustion", in Chemical Kinetics of Small Organic Radicals, Z. Alfassi ed., in press (1987).

29. Slagle, I.R., Park, J.Y., Gutman, D., "Experimental Investigation of the Kinetics and Mechanism of the Reaction of n-Propyl Radicals with Molecular Oxygen from 297 K to 653 K", Twentieth Symposium (International) on Combustion, p. 91, The Combustion Institute, Pittsburgh (1984).

30. Baldwin, R.R., Dean, C.E., and Walker, R.W., "Relative Rate Study of the Addition of HO_2 Radicals to C_2H_4 and C_3H_6", J. Chem. Soc., Faraday Trans. 2, 82 1445 (1986).

31. Walker, R.W. Reaction Kinetics, Royal Society of Chemistry Specialist Periodical Report, Vol. 1, 1961.

32. Baker, R.R., Baldwin, and Walker, R.W., "Addition of n-C_4H_{10} and C_4H_8 to Slowly Reacting Mixtures of Hydrogen and Oxygen at 480°C. Part 2. - Formation of Oxygenated Products," J. Chem. Soc. Faraday Trans. I 71, 756 (1975).

33. Slagle, I.R., Ratajczak, E., Heaven, M.C., Gutman, D. and Wagner, A.F., "Kinetics of Polyatomic Free Radicals Produced by Laser Photolysis. 4. Study of the Equilibrium i-C_3H_7 + O_2 = i-$C_3H_7O_2$ between 592 and 692 K," J. Am. Chem. Soc.107, 1838 (1985).

34. Benson, S.W. Thermochemical Kinetics, Wiley, New York, 1976.

35. Morgan, C.A., Pilling, M.J., Tulloch, J.M., Ruiz, R.P., and Bayes, K.D., "Direct Determination of the Equilibrium Constant and Thermodynamic Parameters for the Reaction C_3H_5+O_2 = $C_3H_5O_2$", J. Chem. Soc., Faraday Trans 2 78, 1323 (1982).

36. Droege, A.T., and Tully, F.P., "Hydrogen-Atom Abstraction from Alkanes by OH. III. Propane", J. Phys. Chem. 90, 1949 (1986).

37. Tully, F.P., J.E.M. Goldsmith, and Droege, A.T., "Hydrogen-Atom Abstraction from Alkanes by OH. III. Iso-butane", J. Phys. Chem. 90, 5932 (1986).

38. Barnard, J.A. and Harwood, B.A., "Slow Combustion and Cool-Flame Behavior of Iso-Octane", Combust. Flame 21, 345 (1973).

39. Baker, R.R., Baldwin, R.R., and Walker, R.W., "Addition of i-Butane to Slowly Reacting Mixtures of Hydrogen and Oxygen at 480 C", J. Chem. Soc. Faraday I 74, 2229 (1978).

40. Benson, S. W., "Effects of Resonance and Structure on the Thermochemistry of Organic Peroxy Radicals and the Kinetics of Combustion Reactions", J. Am. Chem. Soc. 87, 972 (1965).

41. Benson, S. W., "The Kinetics and Thermochemistry of Chemical Oxidation with Application to Combustion and Flames", Prog. Energy Combust. Sci. 7, 125 (1981).

42. Burcat, A., Scheller, K., and Lifshitz, A., "Shock-Tube Investigation of Comparative Ignition Delay Times for C_1-C_5 Alkanes", Combust. Flame 16, 29 (1971).

43. Westbrook, C.K., "An Analytical Study of the Shock Tube Ignition of Mixtures of Methane and Ethane", Combust. Sci. Technol. 20, 5 (1979).

44. Dryer, F.L., and Glassman, I., "High-Temperature Oxidation of CO and CH_4", Fourteenth Symposium (International) on Combustion, p. 987, The Combustion Institute, Pittsburgh (1973).

45. Westbrook, C. K., Creighton, J., Lund, C., and Dryer, F., "A numerical model of chemical kinetics of combustion in a turbulent flow reactor", J. Phys. Chem. 81, 2542 (1977).

46. Kaiser, E.W., Westbrook, C.K., and Pitz, W.J., "Acetaldehyde Oxidation in the Negitive Temperature Coefficient Regime: Experimental and Modeling Results", Int. J. Chem. Kin. 18, 655 (1986).

47. Wilk, R.D., Cernansky, N.P., Pitz, W.J., and Westbrook, C.K., "Propene Oxidation at Low and Intermediate Temperatures: A Detailed Chemical Kinetic Study", Presented at the Western States Section/The Combustion Institute 1987 Spring Meeting, Provo, UT, 6-7 April 1987.

48. Wilk, R.D., Cernansky, N.P., and Cohen, R.S., "An Experimental Study of Propene Oxidation at Low and Intermediate Temperatures", Combust. Sci. Technol. 52, 39 (1987).

49. Griffiths, J.F., "The Fundamentals of Spontaneous Ignition of Gaseous Hydrocarbons and Related Organic Compounds", Adv. Chem. Phys. 64, 203 (1986).

50. Lignola, P.G., and Reverchon, E., "Cool Flames", Prog. Energy Combust. Sci. 13, 75 (1987).

51. Lignola, P.G., Reverchon, E., Autuori, R., Insola, A., and Silvestre, A.M., "Propene Combustion Process in a CSTR", Combust. Sci. Technol. 44, 1 (1985).

52. Frank, J., Griffiths, J.F, and Nimmo, W., "The Control of Spontaneous Ignition under Rapid Compression", Twenty-First Symposium (International) on Combustion, The Combustion Institute, Pittsburgh, in press (1987).

53. Griffiths, J.F., and Hasko, S.M., "Two-Stage Ignitions during Rapid Compression: Spontaneous Combustion in Lean Fuel-Air Mixtures", Proc. R. Soc. Lond. A 393, 371 (1984).

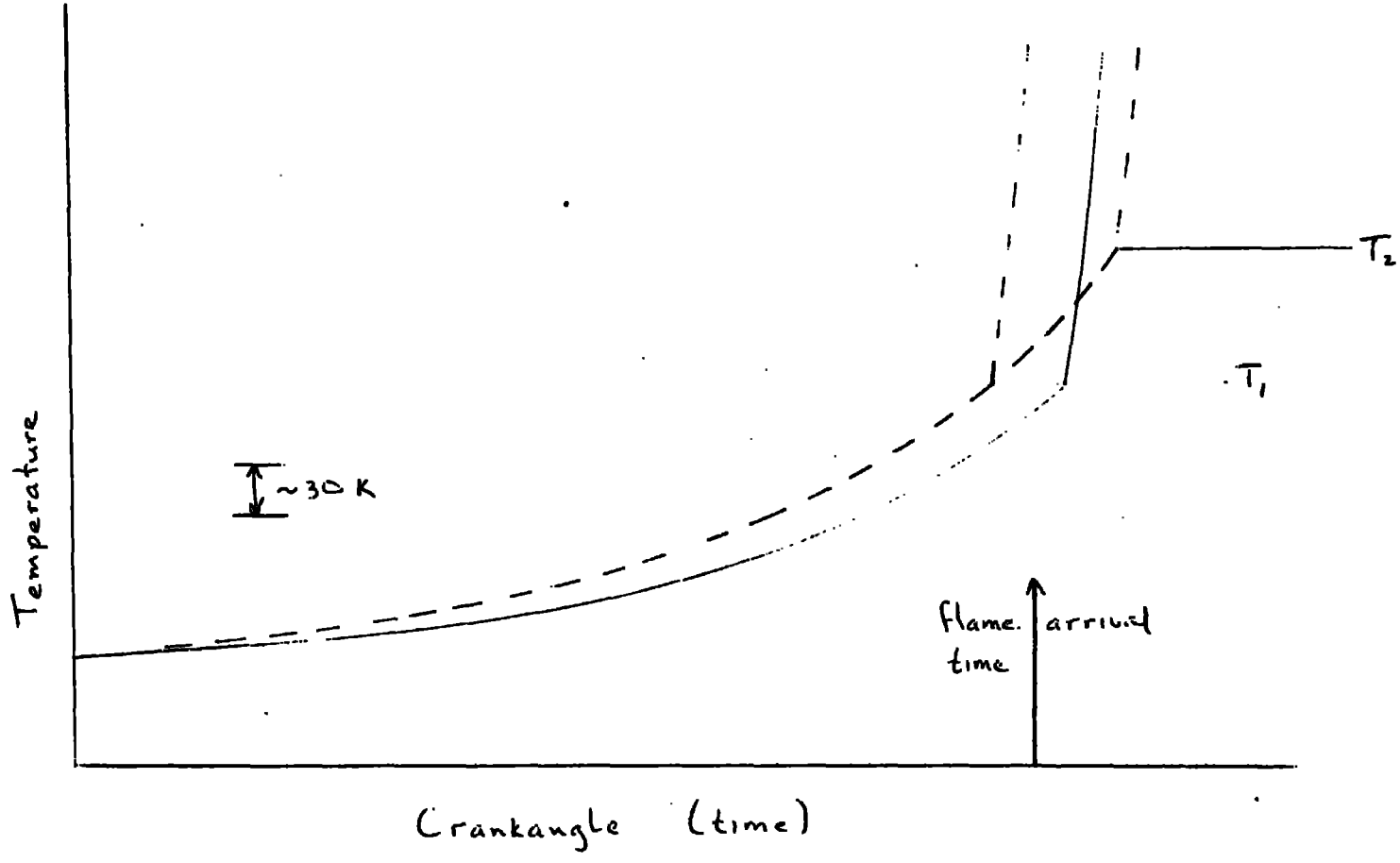

Fig 1. End gas temperature histories

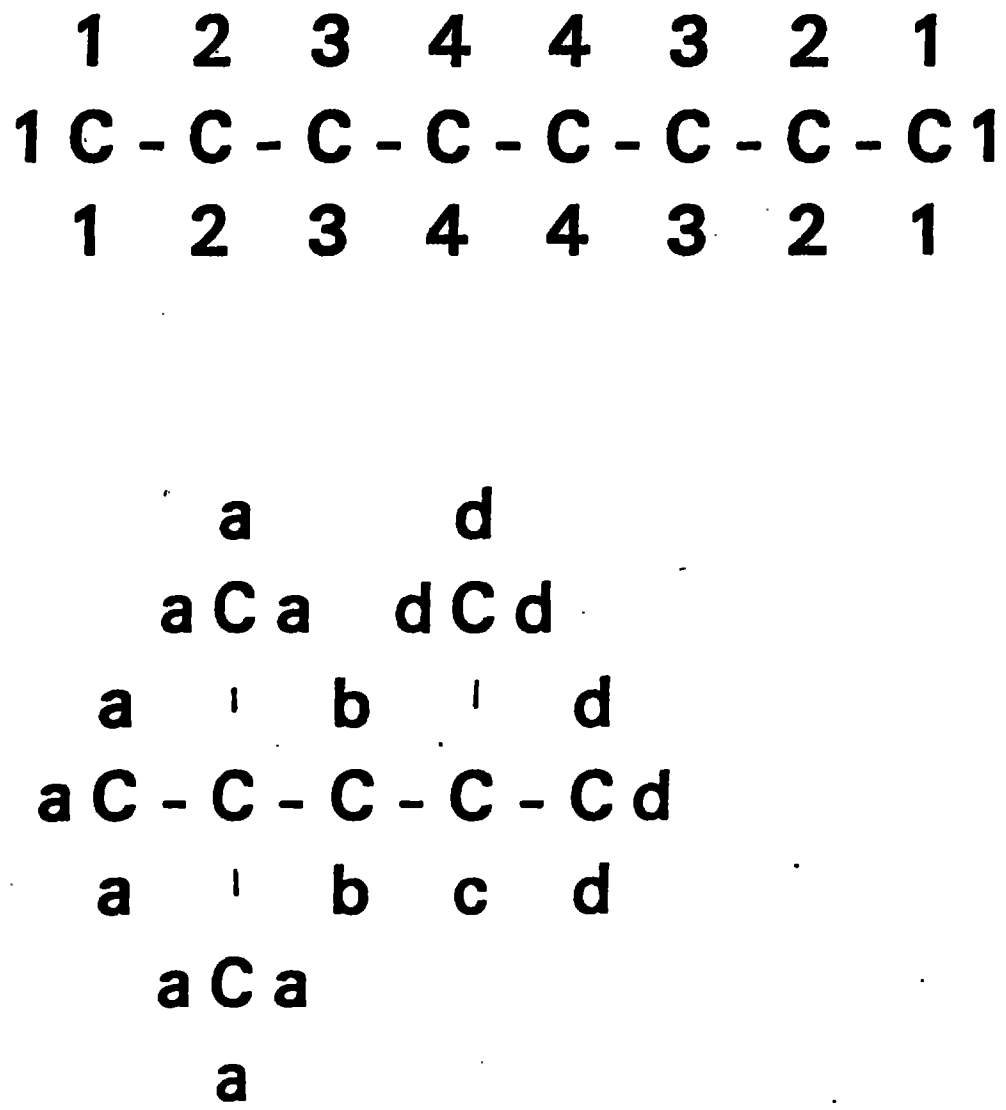

Figure 2. Schematic diagram of n-octane and iso-octane. Numbers in the n-octane and lower case letters in the iso-octane denote logically distinct H atoms

Figure 3. Schematic diagram of two isomers of butane

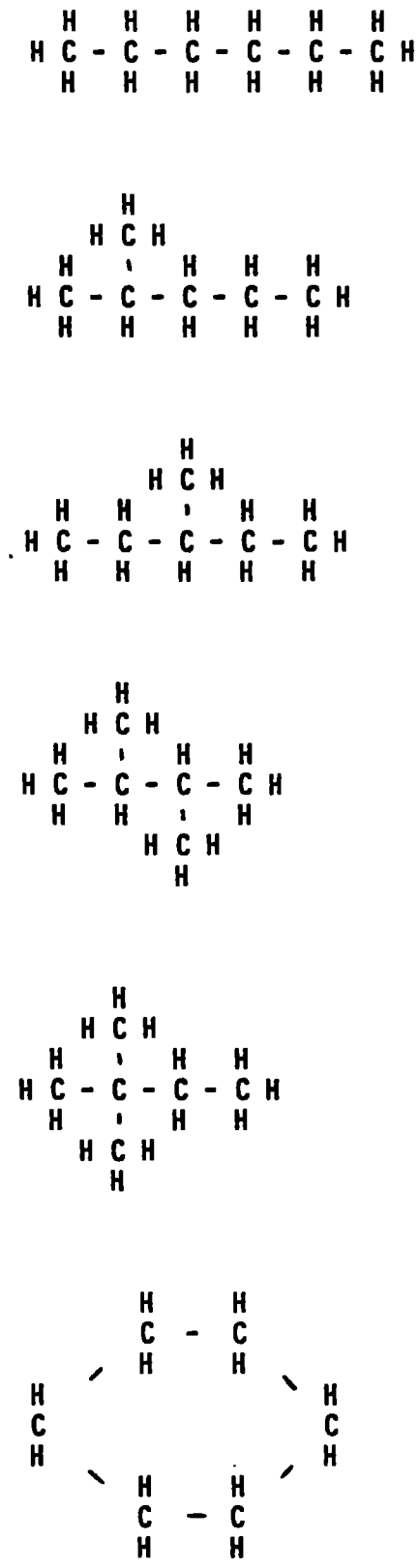

Figure 4. Schematic diagrams for hexane isomers

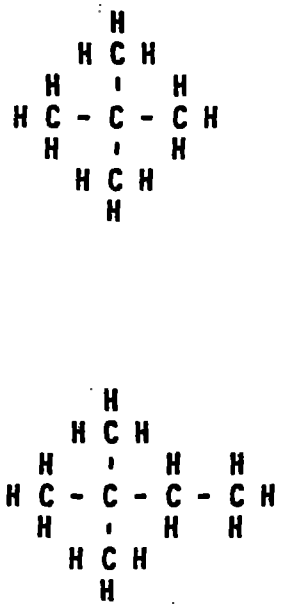

Figure 5. Schematic diagram for neopentane and 2-2 dimethyl butane

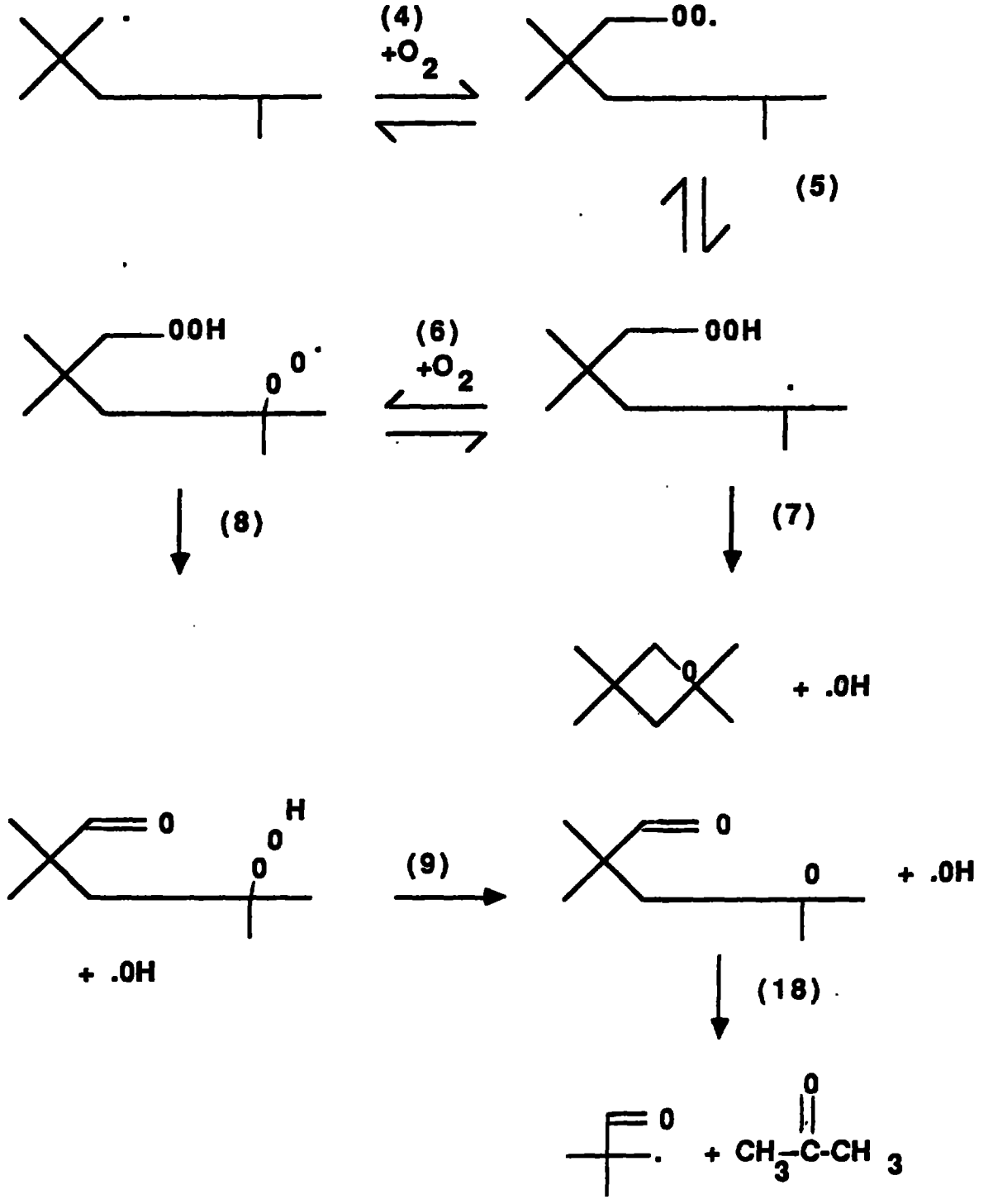

Figure 6. Internal H-atom abstraction of the a-iso-octyl peroxy radical.

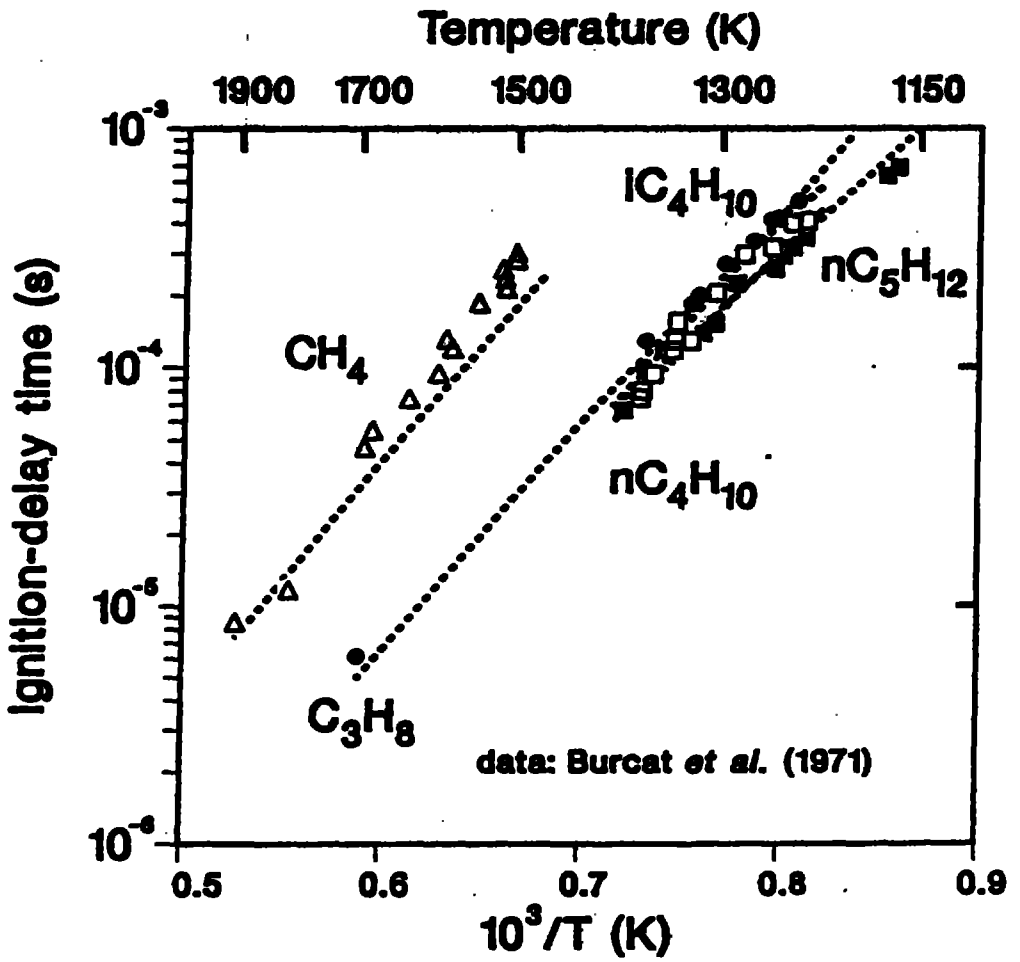

Figure 7. Experimental shock tube ignition delay time measurements [42] (indicated by symbols) and predicted model results for methane, propane, n-butane, and n-pentane. Also shown are computed predictions for iso-butane

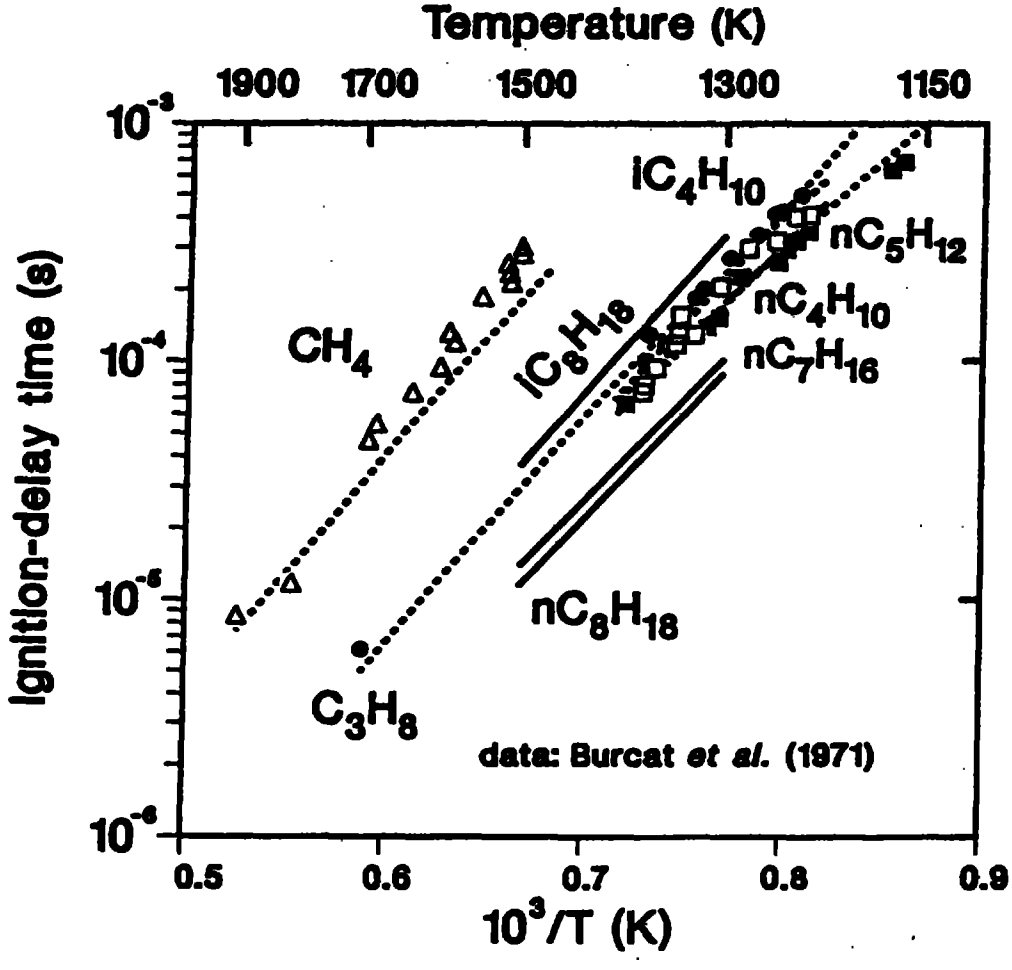

Figure 8. Computed ignition delay times for n-octane, n-heptane, and iso-octane, shown as solid lines, together with some of the experimental and model results from Figure 7 for comparison.